water

MDPI

Article

# Response and Modeling of Hybrid Maize Seed Vigor to Water Deficit at Different Growth Stages

**Rongchao Shi [1], Ling Tong [1], Taisheng Du [1,*] and Manoj K. Shukla [2]**

[1] Center for Agricultural Water Research in China, China Agricultural University, No. 17 Qing-hua East Road, Haidian District, Beijing 100083, China; B20163090567@cau.edu.cn (R.S.); tongling2001@cau.edu.cn (L.T.)
[2] Department of Plant and Environmental Sciences, New Mexico State University, Las Cruces, NM 88003, USA; shuklamk@nmsu.edu
* Correspondence: dutaisheng@cau.edu.cn; Tel.: +86-10-62738398

Received: 4 October 2020; Accepted: 20 November 2020; Published: 23 November 2020


**Abstract:** Research is imperative to predict seed vigor of hybrid maize production under water deficit in arid areas. Field experiments were conducted in 2018 and 2019 in arid areas of northwestern China to investigate the effects of different irrigation strategies at various growth stages with drip irrigation under film mulching on grain yield, kernel weight, seed protein content, and seed vigor of hybrid maize (*Zea mays* L.). Water deficit at vegetative, flowering, and grain-filling stages was considered and a total of 16 irrigation treatments was applied. A total of 12 indices of germination percentage, germination index (GI), shoot length (SL), and root length (RL) under different germination conditions (standard germination and accelerated aging); electrical conductivity (EC) of the leachate; and activities of peroxidase, catalase, and superoxide dismutase in seeds were measured and analyzed using the combinational evaluation method (CEM). Furthermore, five water production functions (Blank, Stewart, Rao, Jensen, and Minhas) were used to predict seed vigor evaluated by CEM under water deficit. The results showed that leachate EC was higher under water deficit than that under sufficient irrigation. The SL, RL, and GI of different germination conditions increased under water deficit at the flowering stage. The Rao model was considered the best fitted model to predict the vigor of hybrid maize seeds under water deficit, and an appropriate water deficit at the flowering stage is recommended to ensure high seed vigor of hybrid maize production with drip irrigation under film mulching. Our findings would be useful for reducing crop water use while ensuring seed vigor for hybrid maize production in arid areas.

**Keywords:** seed quality; maize management; irrigation; water stress

## 1. Introduction

Hybrid maize was commercially grown for the first time in the early 1930s in the United States [1]. Hybrid maize lines show increased yield and disease resistance compared with parental lines, and over 95% of the corn-growing regions worldwide cultivate hybrid maize varieties [2]. With the expansion of the area under cultivation of this crop, the production of hybrid maize seeds has rapidly increased globally. Notably, hybrid maize seed production requires suitable environmental conditions, such as temperature and moisture, as well as technical and professional expertise for industrial production [3]. Over 60% of the total hybrid maize seed production in the world occurs in China (23%), India (15%), the United States (9%), Brazil (5%), Mexico (5%), and Argentina (4%) [4].

Seed vigor involves the combination of all traits that determine the potential activity and performance of seeds during germination and establishment [5]. High seed vigor significantly increases grain yield [6]. Seed vigor tests are divided into physiological methods, which measure germination characteristics, and biochemical methods, which measure specific biochemical reactions

related to seed vigor, such as enzyme activity [7]. The International Seed Testing Association (ISTA) has recommended seven methods for measuring seed vigor, which include the following: electrical conductivity, accelerated aging, cold, controlled deterioration, Hiltner test, seedling growth, and tetrazolium tests [8]. However, there are no universal standardized methods for testing the vigor of maize seeds. The standard germination (SG) test is used to simulate early germination conditions in the field, which are closely associated with field performance [9]. The accelerated aging (AA) test can predict seed storability [10,11]. A previous study has demonstrated a significant negative correlation between the electrical conductivity (EC) of seed leachate and field emergence [12]. In particular, activity of the enzymes superoxide dismutase (SOD), catalase (CAT), and peroxidase (POD) is closely linked to seed vigor [13]. Therefore, it is difficult to determine seed vigor using a single test or vigor index [14–16].

Water is an essential factor for mother plant growth, thereby affecting seed vigor [17–22]. Therefore, water deficit is a key factor in the development of hybrid maize seed production industry. In recent years, water and fertilizer integration through drip irrigation under mulch films has been widely used. Unlike conventional maize, hybrid maize produces high-quality seeds. Therefore, research focusing on the effects of water deficit on seed vigor is imperative to ensure high yield and quality of hybrid maize seeds. Many studies have examined the effects of water deficit on hybrid maize seed yield [23–26]. However, only a few studies have assessed hybrid maize seed vigor under water deficit in the mother plant. Ghassemigolezani et al. [27] found that water deficit during the whole-plant growth stage did not affect seed germination or vigor, although it did markedly affect seed yield. Eskandari et al. [22] found that 50% water deficit with partial root-zone irrigation during various growth stages decreased the germination percentage (GP), shoot length (SL), root length (RL), and seedling dry weight. In a study by Takele and Farrant [28], GP decreased by approximately 80% and 69% and accelerated aging GP decreased by approximately 84% and 67% under lack of irrigation during the pre- and post-flowering stages, respectively, compared with values under sufficient irrigation. Ghassemi-Golezani et al. [29] found that water stress at different growth stages increased EC but decreased GP and seedling dry weight. Baber et al. [30] showed that GP decreased with decreased total irrigation volume at the late growth stage of maize growth. Therefore, it is imperative to develop an irrigation schedule to ensure seed vigor of hybrid maize under water deficit.

Seed vigor is a complex trait, but seed vigor indices have not been comprehensively evaluated to date. Principal component analysis (PCA) and grey relational analysis (GRA) have been adopted to evaluate fruit quality [31,32]. Both methods have specific advantages and disadvantages. Wang [33] integrated the results of different evaluation methods to achieve complementary advantages using a combinational evaluation method (CEM). In this study, we used the CEM to evaluate seed vigor of hybrid maize under water deficit at different growth stages. Meanwhile, the weights of seed vigor indices were determined by the entropy weight method [34].

The crop water production function is often used to simulate the association between crop yield and evapotranspiration at different growth stages. In recent years, the crop water production function has been used to simulate other crop traits. Wang et al. [35] developed specific crop water production functions to predict flowering characteristics of hybrid maize under water deficit at different growth stages. Jiang et al. [36] used the forms of water production functions to model the relationships of tomato relative yield parameters with relative evapotranspiration at each growth stage. In addition, many studies have investigated maize yield and its associated components in response to water deficit [37,38]. However, the association between seed vigor and water deficit during different growth stages of hybrid maize has not been examined in the field. To this end, in the present study, crop water production functions were developed to simulate the vigor of hybrid maize seeds under water deficit at different growth stages. The objectives were to (i) explore the responses of seed yield, kernel weight, and seed protein content to water deficit; (ii) evaluate seed vigor under water deficit at different growth stages; and (iii) establish a water–seed vigor model to predict seed vigor under different irrigation

managements. Our research will create a foundation for developing an irrigation strategy for hybrid maize production to ensure both yield and seed vigor under limited water availability in arid regions.

## 2. Materials and Methods

### 2.1. Experimental Site

The experiments were conducted from April to September in 2018 and 2019 at Shiyanghe Experimental Station of China Agricultural University, Wuwei, Gansu Province, northwestern China (37°52′ N, 102°50′ E; altitude 1581 m). The experimental site has a typical continental temperate climate, with annual average temperature of 8.8 °C, mean sunshine duration of 3000 h, and a frost-free period of 150 d. Annual mean precipitation is 50–150 mm, and annual mean evaporation is 1500–2500 mm [39]. The groundwater table is below 25 m. The experimental site has light sandy loam soil, with a mean soil dry bulk density of 1.38 g $cm^{-3}$, field water capacity of 0.29 $cm^3$ $cm^{-3}$, wilting point of 0.12 $cm^3$ $cm^{-3}$, organic matter content of 0.74%, and available nitrogen content of 23.4 mg $kg^{-1}$ in the 0–1 m soil layer. The available phosphate content is 13.5 mg $kg^{-1}$ and the available potassium content is 103.1 mg $kg^{-1}$ in the 0–40 cm soil layer.

### 2.2. Crop Management

Before sowing, all plots were fertilized with 100 kg $ha^{-1}$ N, 225 kg $ha^{-1}$ $P_2O_5$, and 60 kg $ha^{-1}$ $K_2O$ as basal fertilizers. After fertilization, the soil surface in each plot was partially covered with a plastic mulch film (0.015 mm thick and 1.2 m wide). The width of bare soil between two strips of mulch film was 0.4 m. Drip-irrigated plots with four plantation rows of hybrid maize were top dressed with 100 kg $ha^{-1}$ N during the vegetative and flowering stages. The spacing between the drip irrigation belts was 0.8 m, the distance between emitters was 0.3 m, and the flow rate was 2.5 L $h^{-1}$. The planting density was 9.75 plants per square meter. To ensure seedling emergence, the female parents were irrigated at 30 mm immediately after sowing under all treatments in both years. Cultivars, planting dates of female parents and first and second batches of male parents, planting proportions, and harvest date are summarized in Table 1. Maize seeds were sown as one row of male parents and six rows of female parents in 2018 and as one row of male parents and five rows of female parents in 2019. The two inbred male batches were planted in the same rows, with six plants each from the first and second batches placed in an alternating pattern. The inbred female lines were detasseled after tassel emergence, and the inbred male lines were cut at the end of the pollination stage. Weed and pest control methods followed local practices.

**Table 1.** Cultivars, planting dates of female parents (FP) and first (MP1) and second (MP2) batches of male parents, planting proportions, and harvest date of hybrid maize seeds in each year.

| Year | Cultivar | Planting Date | | | Planting Proportion | | Harvesting Date |
|---|---|---|---|---|---|---|---|
| | | FP | MP1 | MP2 | MP:FP [1] | MP1:MP2 [2] | |
| 2018 | TRF2018 | 18 April | 26 April | 2 May | 1:6 | 6:6 | 17 September |
| 2019 | JDD1903 | 17 April | 1 May | 8 May | 1:5 | 6:6 | 17 September |

[1] Planting proportion of MP and FP in rows. [2] MP1 and MP2 were planted in the same rows, with six plants each from MP1 and MP2 placed in an alternating pattern.

### 2.3. Experimental Design

The growth of hybrid maize over the cropping cycle and seed production was divided into five stages: seedling, vegetative, flowering, grain-filling, and maturity stage. The vegetative stage lasted from the six-leaf stage to before the tasseling of inbred female lines, and the flowering stage lasted from the tasseling of inbred female lines to the end of pollination. A total of 16 treatments were delivered in each year (Table 2). A randomized block design with three replicates per irrigation treatment was used. The experimental plot was 4.8 m wide and 46 m long, and a buffer area (6 m wide and 46 m long)

separated different treatments. The inbred female lines were planted in the buffer zones. In this study, we assumed that the irrigation efficiency is 1, and the irrigation depth per event of sufficient irrigation treatment ($I$) was calculated as follows:

$$I = K_c \times \sum_{i=1}^{n} ET_{0i} - P_e \quad (1)$$

where $ET_{0i}$ is the reference evapotranspiration at the $i$th day in a given irrigation period (mm) (calculated according to the United Nations Food and Agriculture Organization (FAO) Penman–Monteith equation [40]); $n$ is the length of the irrigation period in days; $P_e$ is the effective precipitation (difference between precipitation per rainfall event and 5 mm) in a given irrigation period (mm); and $K_c$ is the crop coefficient in different growth stages.

**Table 2.** Irrigation depth (mm) and times under different irrigation treatments at the seedling (S), vegetative (V), flowering (F), grain-filling (G), and maturity (M) stages of hybrid maize seed production in 2018 and 2019.

| Treatment | 2018 | | | 2019 | | |
|---|---|---|---|---|---|---|
| | V | F | G | V | F | G |
| V2F2G2 [1] | 125 (3) [2] | 85 (3) | 29 (3) | 82 (3) | 60 (2) | 134 (4) |
| V2F2G1 | 125 (3) | 85 (3) | 15 (3) | 82 (3) | 60 (2) | 67 (4) |
| V2F2G0 | 125 (3) | 85 (3) | 0 | 82 (3) | 60 (2) | 0 |
| V2F1G2 | 125 (3) | 43 (3) | 29 (3) | 82 (3) | 30 (2) | 134 (4) |
| V2F1G1 | 125 (3) | 43 (3) | 15 (3) | 82 (3) | 30 (2) | 67 (4) |
| V2F1G0 | 125 (3) | 43 (3) | 0 | 82 (3) | 30 (2) | 0 |
| V2F0G2 | 125 (3) | 0 | 29 (3) | 82 (3) | 0 | 134 (4) |
| V2F0G1 | 125 (3) | 0 | 15 (3) | 82 (3) | 0 | 67 (4) |
| V1F2G2 | 63 (3) | 85 (3) | 29 (3) | 41 (3) | 60 (2) | 134 (4) |
| V1F2G1 | 63 (3) | 85 (3) | 15 (3) | 41 (3) | 60 (2) | 67 (4) |
| V1F2G0 | 63 (3) | 85 (3) | 0 | 41 (3) | 60 (2) | 0 |
| V1F1G2 | 63 (3) | 43 (3) | 29 (3) | 41 (3) | 30 (2) | 134 (4) |
| V1F1G1 | 63 (3) | 43 (3) | 15 (3) | 41 (3) | 30 (2) | 67 (4) |
| V1F1G0 | 63 (3) | 43 (3) | 0 | 41 (3) | 30 (2) | 0 |
| V1F0G2 | 63 (3) | 0 | 29 (3) | 41 (3) | 0 | 134 (4) |
| V1F0G1 | 63 (3) | 0 | 15 (3) | 41 (3) | 0 | 67 (4) |

[1] 2, sufficient irrigation; 1, 50% sufficient irrigation; 0, no irrigation. [2] Numbers between parentheses indicate irrigation events at each growth stage.

In Equation (1), $K_c$ values were 0.33, 0.90, 1.10, 1.02, and 0.80 at the seedling, vegetative, flowering, grain-filling, and maturity stages, respectively [41]. And $ET_{0i}$ was calculated by meteorological data in 2018 and 2019. Under the control treatment (V2F2G2), the maize inbred lines were irrigated every 10 days starting from 5 June 2018 and 4 June 2019, which followed local practices. The two irrigation levels applied at the vegetative stage were 100% $I$ and 50% $I$, and the three irrigation levels applied at the flowering and grain-filling stages were 100% $I$, 50% $I$, and 0 $I$. Because the local hybrid maize cultivars are no irrigated at the seedling and maturity stages, no irrigation treatments were applied at these two stages. The irrigation treatments, depth, and times during different growth stages are presented in Table 2.

Meteorological data were gathered by an automatic weather station (Hobo, Onset Computer Corp., Bourne, MA, USA) about 50 m away from the experimental field and logged every 15 min. The meteorological data of all growth stages in both years are presented in Table 3.

**Table 3.** Daily average solar radiation ($R_s$), air temperature ($T_a$), relative humidity (RH), wind speed ($S_w$), vapor pressure deficit (VPD), reference evapotranspiration ($ET_0$), and total precipitation ($P_{tot}$) at all growth stages in 2018 and 2019.

| Year | Stage | Period | $R_s$ W m$^{-2}$ | $T_a$ °C | VPD k Pa | RH % | $S_w$ m s$^{-1}$ | $P_{tot}$ mm | $ET_0$ mm d$^{-1}$ |
|---|---|---|---|---|---|---|---|---|---|
| 2018 | Seedling | 5 May to 4 June | 241.1 | 17.9 | 1.66 | 41.0 | 0.79 | 5 | 4.14 |
| | Vegetative | 5 June to 4 July | 232.2 | 21.6 | 1.56 | 53.5 | 0.62 | 14 | 4.17 |
| | Flowering | 5 to 30 July | 234.9 | 23.0 | 1.58 | 61.3 | 0.53 | 23 | 4.25 |
| | Grain-filling | 31 July to 1 September | 176.3 | 21.1 | 0.96 | 73.3 | 0.46 | 134 | 3.14 |
| | Maturity | 2 to 16 September | 165.6 | 15.4 | 0.87 | 67.1 | 0.36 | 8 | 2.46 |
| 2019 | Seedling | 4 May to 3 June | 243.8 | 15.9 | 1.34 | 48.3 | 1.03 | 15 | 4.07 |
| | Vegetative | 4 June to 13 July | 232.8 | 20.3 | 1.26 | 62.4 | 0.47 | 72 | 3.95 |
| | Flowering | 14 June to 2 August | 238.3 | 22.0 | 1.61 | 59.3 | 0.27 | 9 | 3.94 |
| | Grain-filling | 3 August to 2 September | 231.1 | 21.3 | 1.62 | 51.8 | 0.32 | 25 | 3.69 |
| | Maturity | 3 to 16 September | 175.5 | 18.3 | 0.95 | 70.4 | 0.25 | 20 | 2.63 |

### *2.4. Sampling and Measurements*

#### 2.4.1. Yield and Yield Components

In each plot, 50 plants of female inbred lines were randomly harvested for yield and kernel weight (KW) measurements. Grains were dried at 105 °C for 30 min and then at 75 °C to a constant weight. A total of 300 grains were randomly selected from each plot and weighted to a constant KW. Seed yield was calculated based on yield per plant and female plant density. Seed yield and KW were converted to weight with kernel water content of 13%. Seed protein content (SPC, Nitrogen × 6.25) was determined using the micro-Kjeldahl method [42].

#### 2.4.2. Evapotranspiration

Soil water content was measured using Diviner 2000 (Sentek Pty Ltd., Adelaide, Australia) within a depth of 1.0 m at 0.1 m intervals every 3–5 d. In addition, soil water content was measured before and after each irrigation and rainfall events. In each plot, one PVC tube was installed under bare soil and another under mulching. A calibration of the Diviner 2000 readings against gravimetric measurements of soil water content was performed for all the tubes separately. Crop evapotranspiration was estimated assuming no water uptake below 1 m, and using the soil water balance method as follows:

$$ET = P_e + I - R - D + CR + \Delta SF - \Delta S \quad (2)$$

where $ET$ is evapotranspiration (mm); $I$ is the total irrigation depth (mm); $R$ is surface runoff (mm); $D$ is deep drainage (mm); $CR$ is capillary rise from a shallow water table towards the root zone (mm); $\Delta SF$ is difference between subsurface flow in and out of the root zone (mm); and $\Delta S$ is the variation in soil water storage (mm).

$\Delta S$ can be calculated as follows:

$$\Delta S = 1000H(W_{t_2} - W_{t_1}) \quad (3)$$

where $W_{t1}$ and $W_{t2}$ are the mean water contents in the root zone at times $t_1$ and $t_2$ (cm$^{-3}$ cm$^{-3}$); and $H$ is soil depth of the planned moisture layer, and here considered as 1 m.

Because some fluxes such as $SF$, $D$ and $CR$ are difficult to assess and short time periods cannot be considered [40]. The experimental site is flat, and surface runoff is not intensive; therefore, $R$ is considered as 0. Therefore, Equation (2) can be simplified as follows:

$$ET = P_e + I - \Delta S \quad (4)$$

#### 2.4.3. Germination Test

For SG test, seeds (100 seeds × 4 replicates) were placed in the germination chamber at 25 °C under 100% relative humidity and 12 h of light per day. Deterioration using AA test is associated with emergence and storage potential. Seeds (100 seeds × 4 replicates) were aged for 72 h at 45 °C under 100% relative humidity. After aging, the seeds were air-dried. GP of SG and AA were evaluated every day until the 7th day according to the recommendations of ISTA [8].

#### 2.4.4. Seedling Growth Test

SLs and RLs of 10 representative seedlings per replicate were measured with a ruler on the 7th day of different germination tests. These indices reflect the robustness of the seedlings.

#### 2.4.5. Germination Index (GI)

GI reflects the germination rate of a seed lot. A higher GI indicates a faster germination rate and can be calculated as follows:

$$\mathrm{GI} = \sum \frac{\mathrm{Gt}}{\mathrm{Dt}} \tag{5}$$

where GI is the germination index; Gt is the number of germinated seeds per day; and Dt is the number of days.

#### 2.4.6. Leachate EC

Approximately 40 g of seeds per replication were soaked in 250 mL of deionized water for 24 h at 25 °C, and the beaker was sealed with plastic wrap. Leachate EC of sample was measured using a conductivity meter (S230, Mettler-Toledo International Inc., Greifensee, Switzerland), and the measurement was repeated four times. The leachate EC per gram of seed weight for each sample can be calculated as follows:

$$\mathrm{EC} = \frac{1}{n} \sum_{i=1}^{n} \frac{S_i - S_0}{m_i}. \tag{6}$$

where EC is the electrical conductivity of leachate per unit mass [μS (cm g)$^{-1}$]; $n$ is the number of repetitions; $S_i$ is the electrical conductivity of the samples (μS cm$^{-1}$); $S_0$ is the electrical conductivity of deionized water (μS cm$^{-1}$); and $m_i$ is the mass of seeds (g).

#### 2.4.7. Enzyme Activity Assay

Two grams of seeds per replication preserved in liquid nitrogen were ground in a mortar and homogenized with 0.4 g polyvinylpyrrolidone in 20 mL of 0.1 M phosphate buffer (pH 7.8) containing 2 mM dithiothreitol, 0.1 mM EDTA and 1.25 mM PEG-4000. The homogenate was centrifuged at 16,000× $g$ for 20 min. The supernatant obtained was used as an enzyme extract. All steps of the extraction procedure were carried out at 1–4 °C. The specific activities of the three enzymes were expressed as units of enzyme activity per milligram of protein, and replicated 15 times per treatment for each enzyme.

SOD activity (U mg$^{-1}$ protein) was assayed by measuring the inhibition of photochemical reduction of nitroblue tetrazolium (NBT) [43]. The reaction mixture contained 75 μM NBT, 13 mM methionie, 2 μM riboflavine, 10 μM EDTA in 0.1 M phosphate buffer (pH 7.8), and 0.1 mL of enzyme extract to a final volume of 3.3 mL. Glass test tubes containing the mixture were placed in a light incubator for 20 min at 25 °C, and the tubes that were not illuminated served as blanks. Absorbance at 560 nm was recorded using a spectrophotometer (UV-2600, Shimadzu Corporation, Kyoto, Germany). A single unit of SOD was defined as the level of enzyme activity required to inhibit the photoreduction of NBT to blue formazan by 50%.

CAT activity (U mg$^{-1}$ protein) was determined according to the method reported by Bailly et al. [13]. Hydrogen peroxide ($H_2O_2$) can be decomposed by CAT, and the absorbance of the reaction solution

decreases with increasing reaction time. The enzyme assay contained 0.1 mM $H_2O_2$ in 50 mM phosphate buffer (pH 7.8) and 0.2 mL of enzyme extract to a final volume of 3 mL. The change in absorbance was recorded using the spectrophotometric method at 240 nm at 30 s intervals. A single unit of CAT activity was defined as a 0.1 change in optical density (OD) per minute.

POD activity (U $mg^{-1}$ protein) was assayed according to the method reported by Shannon et al. [44]. Under POD catalysis, hydrogen peroxide oxidizes guaiacol to form a brown product. The enzyme assay contained 19 µL guaiacol, 30% $H_2O_2$ of 28 µL in 0.2 mM phosphate buffer (pH 6.0) and 1mL enzyme extract to a final volume of 4 mL. The change in absorbance was recorded using spectrophotometry at 470 nm at 30 s intervals. A single unit of POD activity was defined as a 0.01 change in OD per minute.

The protein content of the enzyme extraction solution was measured using Coomassie brilliant blue staining [45], and bovine serum albumin was used as the standard for setting up the calibration curves.

### 2.5. Assessment Methods

In this study, a total of 12 seed vigor indices (GP, GI, SL, and RL under SG and AA conditions, EC, POD, SOD and CAT) were evaluated by GRA, PCA and CEM. PCA and CEM were performed described elsewhere [31,36], and GRA is calculated by the following steps.

(1) Normalize the seed vigor index. The normalized value of the-smaller-the-better index (EC) is expressed as follows:

$$x_{ij} = \frac{y_{j\max} - y_{ij}}{y_{j\max} - y_{j\min}} \tag{7}$$

The normalized values of the-greater-the-better indices (remaining 11 indices) are expressed as follows:

$$x_{ij} = \frac{y_{ij} - y_{j\min}}{y_{j\max} - y_{j\min}} \tag{8}$$

where $x_{ij}$ is normalized value of seed vigor index; $y_{ij}$ is the original seed vigor index; $i = 1, 2, \ldots, m$; $j = 1, 2, \ldots, n$; $y_{j\max}$ is the maximum value of the $j$th index; and $y_{j\min}$ is the minimum value of the $j$th index. In this study, $m = 16$ and $n = 12$.

(2) The grey relational coefficient ($\xi_{ij}$) is calculated as follows:

$$\xi_{ij} = \frac{\min\limits_i \min\limits_j \left|x_j^0 - x_{ij}\right| + \rho \min\limits_i \min\limits_j \left|x_j^0 - x_{ij}\right|}{\left|x_j^0 - x_{ij}\right| + \rho \min\limits_i \min\limits_j \left|x_j^0 - x_{ij}\right|} \tag{9}$$

where $x_j^0$ is the ideal normalized result for the $j$th index; and $\rho = 0.5$.

(3) The weighted grey relational grade for the $i$th treatment ($R_i^*$) is calculated as follows:

$$R_i^* = \sum_{i=1}^{m} W_X \xi_{ij} \tag{10}$$

where $W_X$ is the weight of each seed vigor index, derived from the entropy method. And the entropy method has been detailed in Ding et al. [34].

### 2.6. Water–Seed Vigor Models

The crop water production functions using the Blank [46], Stewart [47], Rao [48], Jensen [49], and Minhas [50] models were applied to simulate the seed vigor of hybrid maize under water deficit in the present study.

Blank model:

$$\frac{V_i}{V_{CK}} = \sum_{a=1}^{3} A_a \left(\frac{ET_{ia}}{ET_{CKa}}\right) \tag{11}$$

Stewart model:

$$\frac{V_i}{V_{CK}} = 1 - \sum_{a=1}^{3} B_a\left(1 - \frac{ET_{ia}}{ET_{CKa}}\right) \tag{12}$$

Rao model:

$$\frac{V_i}{V_{CK}} = \prod_{a=1}^{3}\left(1 - C_a\left(1 - \frac{ET_{ia}}{ET_{CKa}}\right)\right) \tag{13}$$

Jensen model:

$$\frac{V_i}{V_{CK}} = \prod_{a=1}^{3}\left(\frac{ET_{ia}}{ET_{CKa}}\right)^{\lambda_a} \tag{14}$$

Minhas model:

$$\frac{V_i}{V_{CK}} = \prod_{a=1}^{3}\left(1 - \left(1 - \frac{ET_{ia}}{ET_{CKa}}\right)^2\right)^{\delta_a} \tag{15}$$

where $V_i$ is the seed vigor under the $i$th treatment evaluated by CEM; $V_{CK}$ is the seed vigor under sufficient irrigation (V2F2G2) evaluated by CEM; $a$ = 1, 2, and 3 indicate the vegetative, flowering, and grain-filling stages, respectively; $ET_{ia}$ is evapotranspiration under the $i$th treatment at the $a$th growth stage (mm); $ET_{CKa}$ is evapotranspiration under sufficient irrigation at the $a$th growth stage (mm); and $\lambda_a$, $\delta_a$, $A_a$, $B_a$, and $C_a$ indicate water sensitivity indices at the $a$th growth stage.

### *2.7. Data Analysis*

Because of high rainfall at the grain-filling stage in 2018, the water–seed vigor models were calibrated using 12 irrigation treatments (V2F2G2, V2F1G0, V2F0G2, V1F2G0, V1F1G1, and V1F0G2 in each year) and validated using the remaining 20 irrigation treatments in 2018 and 2019.

SPSS 21.0 (SPSS Inc., USA) was used for the one-way analysis of variance, verification normality and homogeneity of variance, and comparison of mean values with the Duncan multiple range tests at a 5% probability level. SAS 9.3 (SAS Institute, USA) was used for PCA and non-linear fitting. Model performance was evaluated based on relative root-mean-square error (RRMSE), coefficient of determination ($R^2$), average relative error (ARE), modeling efficiency (EF), and agreement index ($d_{\mathrm{IA}}$). The equations for computing these indicators are the following:

$$b = \frac{\sum_{i=1}^{n} M_i P_i}{\sum_{i=1}^{n} M_i^2} \tag{16}$$

$$\mathrm{RRMSE} = \frac{1}{\overline{M}}\sqrt{\frac{1}{n}\sum_{i=1}^{n}(P_i - M_i)^2} \tag{17}$$

$$R^2 = \left[\frac{\sum_{i=1}^{n}\left(P_i - \overline{P}\right)\left(M_i - \overline{M}\right)}{\sqrt{\sum_{i=1}^{n}\left(P_i - \overline{P}\right)^2 \sum_{i=1}^{n}\left(M_i - \overline{M}\right)^2}}\right]^2 \tag{18}$$

$$\mathrm{ARE} = \frac{\sum_{i=1}^{n}|P_i - M_i|}{n\overline{M}} \tag{19}$$

$$\mathrm{EF} = 1 - \frac{\sum_{i=1}^{n} (P_i - M_i)^2}{\sum_{i=1}^{n} \left(M_i - \overline{M}\right)^2} \quad (20)$$

$$d_{IA} = 1 - \frac{\sum_{i=1}^{n} (P_i - M_i)^2}{\sum_{i=1}^{n} \left(\left|P_i - \overline{M}\right| + \left|M_i - \overline{P}\right|\right)^2} \quad (21)$$

where $n$ is the sample size; $P_i$ is the predicted value; $M_i$ is the measured value; $\overline{P}$ is the mean of the predicted values; and $\overline{M}$ is the mean of the measured values.

## 3. Results and Discussion

### *3.1. Soil Water Content, Evapotranspiration, Yield, Kernel Weight, and Seed Protein Content*

Figure 1 shows the trends of mean soil volumetric water content in the 0–1 m soil layer under different irrigation treatments in 2018 and 2019. In this study, the lower limit of readily available water was 0.20 $cm^{-3}$ $cm^{-3}$ [40]. Soil water contents in all treatments were significantly affected by irrigation and rainfall, and fluctuated differently between the wilting point and field capacity, and decreased with the reduction of irrigation depth at different growth stages.

There were no significant differences on all the indices among the different irrigation treatments at the grain-filling stage in 2018 due to heavy rainfall (Table 3). ET, yield, KW, and SPC of hybrid maize seeds under different treatments are presented in Table 4. Compared with the value under V2F2G2, ET declined by 41.0% under V1F0G1 in 2018 and by 43.4% under V1F1G0 in 2019. Water deficit at different growth stages significantly decreased yield in both years. Consequently, the yield decreased by 73.0% and 78.7% under V1F0G1 in 2018 and 2019.

**Table 4.** Evapotranspiration (ET), yield, kernel weight (KW), and seed protein content (SPC) of hybrid maize seeds under different irrigation treatments in 2018 and 2019.

| Treatment | 2018 | | | | 2019 | | | |
|---|---|---|---|---|---|---|---|---|
| | ET mm | Yield t ha$^{-1}$ | KW mg | SPC % | ET mm | Yield t ha$^{-1}$ | KW mg | SPC % |
| V2F2G2 [1] | 437 [a,2] | 5.04 [a] | 385.3 [b] | 10.76 [c] | 531 [a] | 4.42 [a] | 345.7 [b] | 11.11 [a] |
| V2F2G1 | 432 [a] | 4.95 [a] | 385.8 [b] | 10.76 [c] | 469 [b,c] | 3.84 [b] | 300.2 [f] | 10.92 [b,c,d] |
| V2F2G0 | 433 [a] | 4.98 [a] | 385.2 [b] | 10.76 [c] | 424 [d,e] | 3.34 [d] | 261.6 [i] | 10.79 [e,f] |
| V2F1G2 | 396 [b] | 4.72 [b] | 387.0 [b] | 10.99 [b] | 476 [b] | 3.11 [e] | 350.3 [b] | 11.14 [a] |
| V2F1G1 | 394 [b] | 4.70 [b] | 387.0 [b] | 10.99 [b] | 416 [e,f] | 2.75 [f] | 309.5 [d,e] | 10.92 [b,c,d] |
| V2F1G0 | 392 [b] | 4.66 [b] | 386.4 [b] | 11.00 [b] | 377 [h] | 2.41 [h] | 271.7 [h] | 10.77 [e,f] |
| V2F0G2 | 364 [c] | 3.82 [d] | 391.9 [a] | 11.24 [a] | 429 [d] | 2.74 [f] | 359.0 [a] | 11.16 [a] |
| V2F0G1 | 364 [c] | 3.80 [d] | 391.1 [a] | 11.21 [a] | 390 [g] | 2.39 [h] | 314.1 [d] | 10.90 [c,d] |
| V1F2G2 | 350 [d] | 4.40 [c] | 359.8 [d] | 10.52 [e] | 459 [c] | 3.57 [c] | 324.8 [c] | 11.01 [b] |
| V1F2G1 | 351 [d] | 4.35 [c] | 360.0 [d] | 10.51 [e] | 412 [f] | 3.10 [e] | 282.0 [g] | 10.84 [d,e] |
| V1F2G0 | 345 [d] | 4.37 [c] | 360.8 [d] | 10.50 [e,f] | 349 [j] | 2.64 [g] | 239.9 [j] | 10.58 [g] |
| V1F1G2 | 316 [e] | 3.46 [e] | 364.8 [c] | 10.72 [d] | 409 [f] | 2.05 [i] | 330.6 [c] | 10.95 [b,c] |
| V1F1G1 | 317 [e] | 3.37 [e] | 364.7 [c] | 10.71 [d] | 362 [i] | 1.60 [j] | 258.5 [i] | 10.83 [d,e] |
| V1F1G0 | 313 [e] | 3.36 [e] | 363.8 [c] | 10.72 [d] | 301 [l] | 1.22 [l] | 197.4 [k] | 10.61 [g] |
| V1F0G2 | 263 [f] | 1.37 [f] | 354.6 [e] | 10.47 [f] | 339 [j] | 1.45 [k] | 306.2 [e,f] | 10.71 [f] |
| V1F0G1 | 258 [f] | 1.36 [f] | 355.0 [e] | 10.48 [ef] | 317 [k] | 0.94 [m] | 199.5 [k] | 10.61 [g] |

[1] V, vegetative; F, flowering; G, grain-filling; 2, sufficient irrigation; 1, 50% sufficient irrigation; 0, no irrigation.
[2] Different letters in columns indicate significant differences among treatments within a year at a 5% probability level using Duncan multiple range test.

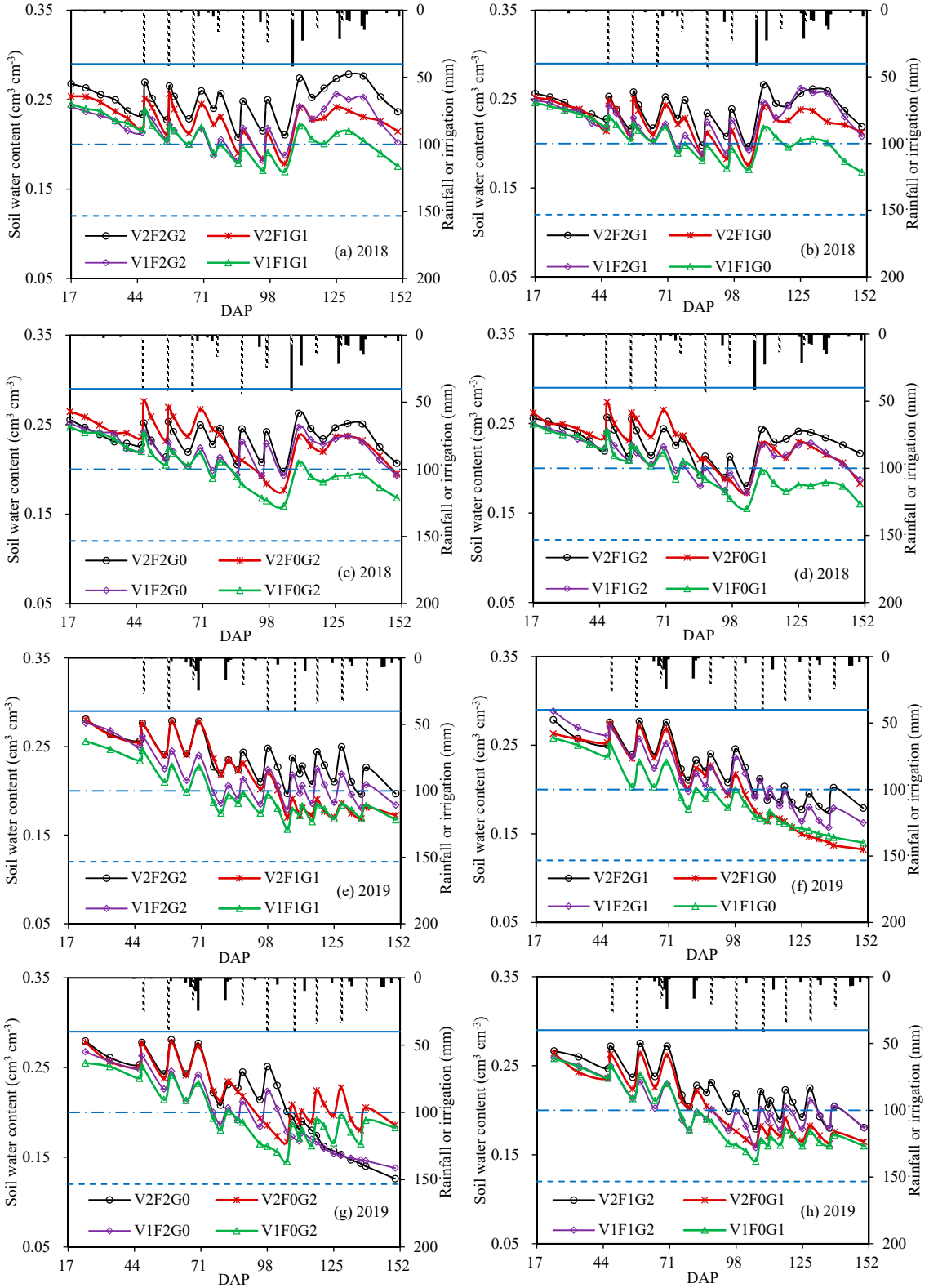


**Figure 1.** Trends of volumetric soil water content during hybrid maize seed production under different treatments in 2018 (**a**–**d**) and 2019 (**e**–**h**). V, vegetative; F, flowering; G, grain-filling; 2, sufficient irrigation; 1, 50% sufficient irrigation; 0, no irrigation; DAP, days after planting; ■ Irrigation of V2F2G2; ▨ rainfall; —— field water capacity; - - - - wilting point; —·— lower limit of readily available water, and here considered as 0.20 $cm^{-3}$ $cm^{-3}$ [40].

KW is an important component of maize yield. In this study, water deficit at the flowering stage significantly increased KW in both 2018 and 2019. This result is consistent with that of the study conducted by NeSmith and Ritchie [51]. In contrast, some studies showed that water deficit at the flowering stage decreased KW [52–54], while others found no effect [24,55,56]. Water deficit at the flowering stage significantly affected flowering characteristics and decreased kernel number [24]. The post-flowering assimilate availability per kernel under water deficit at the flowering stage may be the reason for increased KW. On the other hand, water deficit at vegetative and grain-filling stage decreased KW as a result of reduced the post-flowering assimilate availability per kernel.

SPC usually decreases with increasing total irrigation volume [57–60]. However, severe water stress delays the growth of leaf and stem cells, affects nutrient transport, and decreases SPC [61–63]. In this study, water deficit at the flowering stage did not significantly affect SPC in 2019, although water deficit at the vegetative and grain-filling stages significantly reduced SPC in both years. Furthermore, compared with the value under V2F2G2, SPC under V2F0G2 increased by 4.5% in 2018. Similar to KW, SPC is typically affected by changes in post-flowering assimilate availability per kernel [64,65]. Therefore, increased post-flowering assimilate availability per kernel under water deficit at the flowering stage may be another reason for increased SPC.

### 3.2. Seed Vigor

Cell membrane damage caused by water stress may increase the EC of seed leachate. Values of leachate EC under different irrigation treatments are shown in Figure 2. The results showed that EC significantly increased under water deficit at different growth stages. This is consistent with findings reported in maize [29] and soybean [18,19,66]. Compared with the value under V2F2G2, EC increased by 47.4% and 47.3% under V1F0G1 in 2018 and 2019, respectively.

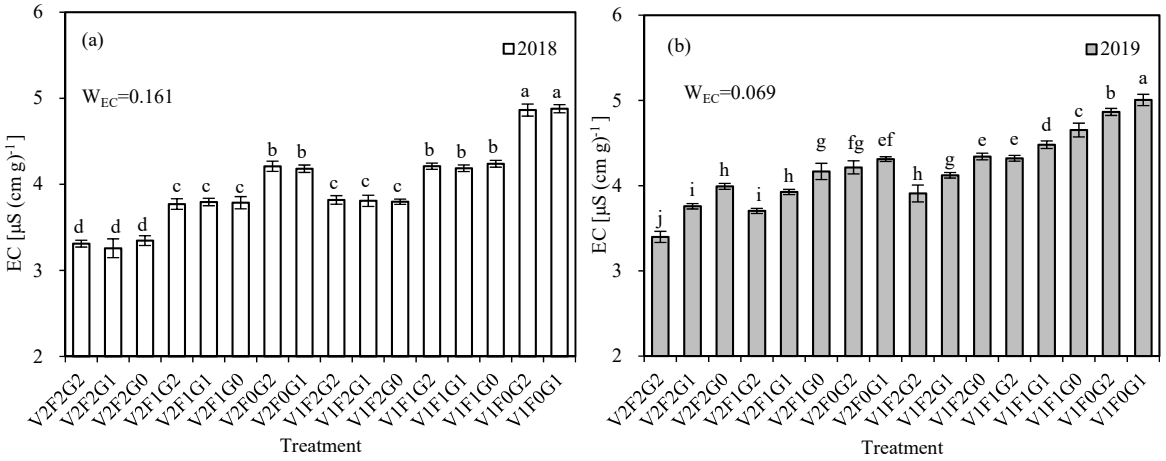


**Figure 2.** Leachate electrical conductivity (EC) and weight of EC determined using the entropy method ($W_{EC}$) in 2018 (**a**) and 2019 (**b**). V, vegetative; F, flowering; G, grain-filling; 2, sufficient irrigation; 1, 50% sufficient irrigation; 0, no irrigation. Inserted error bars denote standard error of the mean. Different letters above error bars indicate significant differences among treatments within a year at a 5% probability level using Duncan multiple range test.

The GP, GI, SL, and RL of SG test under different irrigation treatments in 2018 and 2019 are provided in Table 5. Water deficit at the flowering stage did not affect $GP_{SG}$, except in V1F0G2 and V1F0G1; however, water deficit at the vegetative and grain-filling stages significantly decreased $GP_{SG}$. Conversely, $SL_{SG}$, $RL_{SG}$ and $GI_{SG}$ decreased with the intensity of water deficit at the vegetative and grain-filling stages but increased with the intensity of water deficit at the flowering stage, particularly under V2F0G2.

**Table 5.** Germination percentage (GP), germination index (GI), seedling length (SL), and root length (RL) on the 7th day of standard germination (SG) test under different irrigation treatments and weight determined using the entropy weight method ($W_X$) in 2018 and 2019.

| Treatment | 2018 | | | | 2019 | | | |
|---|---|---|---|---|---|---|---|---|
| | $GP_{SG}$ % | $GI_{SG}$ | $SL_{SG}$ cm | $RL_{SG}$ cm | $GP_{SG}$ % | $GI_{SG}$ | $SL_{SG}$ cm | $RL_{SG}$ cm |
| V2F2G2 [1] | 97.8 [a,2] | 36.79 [c,d] | 9.1 [c,d] | 26.9 [c] | 98.5 [a] | 32.09 [c] | 10.6 [c] | 30.2 [b] |
| V2F2G1 | 98.0 [a] | 36.79 [c,d] | 9.0 [c,d] | 26.8 [c] | 94.3 [c] | 30.70 [e] | 9.7 [f] | 29.0 [d] |
| V2F2G0 | 98.0 [a] | 36.77 [d] | 8.9 [d] | 26.8 [c] | 92.5 [e] | 29.19 [g] | 8.8 [h] | 26.3 [g] |
| V2F1G2 | 97.9 [a] | 37.03 [b] | 10.0 [b] | 27.5 [b] | 98.3 [a] | 32.72 [b] | 11.0 [b] | 31.3 [a] |
| V2F1G1 | 97.5 [a] | 36.96 [b,c] | 10.0 [b] | 27.4 [b] | 94.8 [b,c] | 31.26 [d] | 10.0 [e,f] | 29.8 [b,c] |
| V2F1G0 | 97.9 [a] | 37.03 [b] | 9.9 [b] | 27.4 [b] | 90.6 [f] | 29.20 [g] | 9.3 [g] | 26.7 [f,g] |
| V2F0G2 | 98.0 [a] | 37.36 [a] | 10.5 [a] | 28.0 [a] | 98.6 [a] | 33.58 [a] | 11.6 [a] | 32.1 [a] |
| V2F0G1 | 97.9 [a] | 37.32 [a] | 10.4 [a] | 28.0 [a] | 94.6 [b,c] | 31.98 [c] | 10.5 [c,d] | 30.1 [b] |
| V1F2G2 | 96.3 [b] | 36.25 [e] | 8.7 [e] | 26.4 [d] | 95.0 [b,c] | 30.72 [e] | 9.7 [f] | 29.0 [d] |
| V1F2G1 | 96.3 [b] | 36.23 [e] | 8.6 [e] | 26.4 [d] | 93.3 [d] | 29.83 [f] | 9.1 [g,h] | 27.7 [e] |
| V1F2G0 | 96.2 [b] | 36.20 [e] | 8.7 [e] | 26.4 [d] | 88.1 [h] | 27.88 [i] | 8.3 [i] | 24.0 [h] |
| V1F1G2 | 96.3 [b] | 36.38 [e] | 9.2 [c] | 26.8 [c] | 95.2 [b] | 31.22 [d] | 10.2 [d,e] | 29.8 [b,c] |
| V1F1G1 | 96.3 [b] | 36.38 [e] | 9.2 [c] | 26.7 [c] | 93.5 [d] | 28.71 [h] | 8.9 [g,h] | 27.2 [e,f] |
| V1F1G0 | 95.9 [b] | 36.29 [e] | 9.2 [c] | 26.8 [c] | 87.9 [h] | 26.77 [j] | 7.8 [j] | 24.5 [h] |
| V1F0G2 | 94.5 [c] | 35.64 [f] | 8.1 [f] | 25.7 [e] | 94.5 [b,c] | 29.95 [f] | 9.8 [e,f] | 29.1 [c,d] |
| V1F0G1 | 94.4 [c] | 35.59 [f] | 8.0 [f] | 25.7 [e] | 89.4 [g] | 27.96 [i] | 8.0 [I,j] | 26.4 [f,g] |
| $W_X$ | 0.067 | 0.070 | 0.089 | 0.079 | 0.088 | 0.071 | 0.089 | 0.073 |

[1] V, vegetative; F, flowering; G, grain-filling; 2, sufficient irrigation; 1, 50% sufficient irrigation; 0, no irrigation. [2] Different letters in columns indicate significant differences among treatments within a year at a 5% probability level using Duncan multiple range test.

There was no significant change in $GP_{SG}$ under water deficit at the flowering stage, except under V1F0G2 and V1F0G1. However, Takele and Farrant [28] found that water deficit at the flowering stage decreased $GP_{SG}$ by 80%. Lieffering et al. [67] reported that the rate and degree of seed imbibition were significantly related to the colloidal properties of seeds. Since proteins are an important colloidal constituent, the germination rate increased with increase in SPC [68]. Moreover, seeds with higher SPC showed a faster rate of transfer of dry matter and N reserves from the endosperm to the embryo to enhance seedling vigor [69–71]. On the other hand, larger seeds tend to produce more vigorous seedlings than smaller seeds [72–74]. Therefore, increases in SPC and KW caused by water deficit at the flowering stage may have increased $GI_{SG}$, $SL_{SG}$ and $RL_{SG}$ in both years.

Deterioration using AA test is associated with emergence and storage potential. The GP, GI, SL, and RL of AA test under different irrigation treatments in 2018 and 2019 are provided in Table 6. The results showed that water deficit at vegetative and grain-filling stages significantly decreased $GP_{AA}$, $GI_{AA}$, $SL_{AA}$, and $RL_{AA}$. This is consistent with findings reported in previous researches [28,75,76]. However, water deficit at the flowering stage significantly increased $GP_{AA}$ in both years. Pedrinho et al. [77] suggested that $GP_{AA}$ was positively correlated with SPC, and in this study, water deficit at the flowering stage increased $GP_{AA}$ by increasing the SPC.

The activities (U $mg^{-1}$ protein) of SOD, CAT, and POD of hybrid maize seeds under different irrigation treatments are listed in Table 7. The results showed that water deficit at the vegetative and grain-filling stages significantly decreased SOD, CAT, and POD. Compared with its effects on SOD activity, water deficit at the flowering stage showed limited effects on CAT and POD activities. Anwar et al. [63] found that the maximum increase in CAT activity in maize grains was observed under drought stress at the grain-filling and silking stages. Eisvand et al. [78] suggested that late drought decreased CAT activity but did not affect POD and SOD activities in wheat grains. Water deficit at the vegetative stage significantly reduced antioxidant enzyme activities, possibly due to the inhibition of enzyme synthesis or change in the assembly of enzyme subunits under water stress [78].

**Table 6.** Germination percentage (GP), germination index (GI), seedling length (SL), and root length (RL) on the 7th day of accelerated aging (AA) test under different irrigation treatments and weight determined using the entropy weight method ($W_X$) in 2018 and 2019.

| Treatment | 2018 | | | | 2019 | | | |
|---|---|---|---|---|---|---|---|---|
| | $GP_{AA}$ % | $GI_{AA}$ | $SL_{AA}$ cm | $RL_{AA}$ cm | $GP_{AA}$ % | $GI_{AA}$ | $SL_{AA}$ cm | $RL_{AA}$ cm |
| V2F2G2 [1] | 79.8 $^{d,2}$ | 26.63 $^{c}$ | 6.8 $^{c}$ | 15.7 $^{c}$ | 74.8 $^{c}$ | 24.66 $^{c}$ | 7.7 b $^{c}$ | 17.3 $^{c}$ |
| V2F2G1 | 79.7 $^{d}$ | 26.58 $^{c,d}$ | 6.7 $^{c}$ | 15.7 $^{c}$ | 72.6 $^{e}$ | 23.98 $^{d}$ | 6.9 $^{e,f}$ | 16.2 $^{d,e}$ |
| V2F2G0 | 79.7 $^{d}$ | 26.58 $^{c,d}$ | 6.8 $^{c}$ | 15.6 $^{c}$ | 70.3 $^{h}$ | 23.11 $^{g}$ | 6.2 $^{g,h}$ | 15.2 $^{f}$ |
| V2F1G2 | 80.3 $^{b}$ | 26.94 $^{b}$ | 7.1 $^{b}$ | 16.2 $^{b}$ | 76.0 $^{b}$ | 25.12 $^{b}$ | 7.9 $^{b}$ | 17.8 $^{b}$ |
| V2F1G1 | 80.2 $^{b,c}$ | 26.88 $^{b}$ | 7.1 $^{b}$ | 16.1 $^{b}$ | 73.6 $^{d}$ | 24.14 $^{d}$ | 7.1 $^{d,e}$ | 16.3 $^{d}$ |
| V2F1G0 | 80.2 $^{b,c}$ | 26.89 $^{b}$ | 7.1 $^{b}$ | 16.1 $^{b}$ | 71.0 $^{g}$ | 23.41 $^{e,f}$ | 6.6 $^{f,g}$ | 15.3 $^{f}$ |
| V2F0G2 | 81.0 $^{a}$ | 27.18 $^{a}$ | 7.7 $^{a}$ | 16.7 $^{a}$ | 78.8 $^{a}$ | 26.10 $^{a}$ | 8.3 $^{a}$ | 18.4 $^{a}$ |
| V2F0G1 | 80.9 $^{a}$ | 27.13 $^{a}$ | 7.6 $^{a}$ | 16.7 $^{a}$ | 69.8 $^{i,j}$ | 22.82 $^{h}$ | 6.2 $^{g,h}$ | 16.6 $^{d}$ |
| V1F2G2 | 79.1 $^{e}$ | 26.32 $^{e}$ | 6.4 $^{d}$ | 15.2 $^{d}$ | 72.0 $^{f}$ | 23.51 $^{e}$ | 6.9 $^{e,f}$ | 15.8 $^{e}$ |
| V1F2G1 | 79.1 $^{e}$ | 26.28 $^{e}$ | 6.3 $^{d}$ | 15.2 $^{d}$ | 70.3 $^{h,i}$ | 23.01 $^{g}$ | 6.6 $^{f,g}$ | 15.2 $^{f}$ |
| V1F2G0 | 79.0 $^{e}$ | 26.28 $^{e}$ | 6.5 $^{d}$ | 15.1 $^{d}$ | 68.0 $^{k}$ | 22.07 $^{i}$ | 5.8 $^{h,i}$ | 14.3 $^{g}$ |
| V1F1G2 | 79.9 $^{b,c,d}$ | 26.56 $^{c,d}$ | 6.8 $^{c}$ | 15.7 $^{c}$ | 73.0 $^{e}$ | 24.14 $^{d}$ | 7.4 $^{c,d}$ | 16.3 $^{d}$ |
| V1F1G1 | 80.0 $^{b,c,d}$ | 26.52 $^{d}$ | 6.7 $^{c}$ | 15.6 $^{c}$ | 70.0 $^{h,i}$ | 22.99 $^{g}$ | 6.1 $^{h}$ | 14.2 $^{g}$ |
| V1F1G0 | 79.8 $^{c,d}$ | 26.52 $^{d}$ | 6.8 $^{c}$ | 15.7 $^{c}$ | 67.3 $^{l}$ | 21.70 $^{j}$ | 5.5 $^{i}$ | 13.5 $^{h}$ |
| V1F0G2 | 78.3 $^{f}$ | 25.90 $^{f}$ | 5.9 $^{e}$ | 14.6 $^{e}$ | 73.0 $^{e}$ | 23.31 $^{f}$ | 7.1 $^{d,e}$ | 16.6 $^{d}$ |
| V1F0G1 | 78.4 $^{f}$ | 25.86 $^{f}$ | 5.8 $^{e}$ | 14.6 $^{e}$ | 69.3 $^{j}$ | 21.92 $^{i}$ | 6.1 $^{h}$ | 14.4 $^{g}$ |
| $W_X$ | 0.069 | 0.069 | 0.071 | 0.079 | 0.092 | 0.096 | 0.082 | 0.079 |

[1] V, vegetative; F, flowering; G, grain-filling; 2, sufficient irrigation; 1, 50% sufficient irrigation; 0, no irrigation. [2] Different letters in columns indicate significant differences among treatments within a year at a 5% probability level using Duncan multiple range test.

**Table 7.** Activities (U $mg^{-1}$ protein) of superoxide dismutase (SOD), catalase (CAT), and peroxidase (POD) of hybrid maize seeds under different irrigation treatments and weight determined using the entropy weight method ($W_X$) in 2018 and 2019.

| Treatment | 2018 | | | 2019 | | |
|---|---|---|---|---|---|---|
| | SOD | CAT | POD | SOD | CAT | POD |
| V2F2G2 [1] | 0.98 $^{a,2}$ | 0.0323 $^{a}$ | 0.0405 $^{a}$ | 1.25 $^{a}$ | 0.0391 $^{a,b}$ | 0.0486 $^{a}$ |
| V2F2G1 | 0.98 $^{a}$ | 0.0319 $^{a,b}$ | 0.0397 $^{a,b,c}$ | 1.16 $^{b,c}$ | 0.0386 $^{a,b}$ | 0.0476 $^{a,b}$ |
| V2F2G0 | 0.97 $^{a,b}$ | 0.0331 $^{a}$ | 0.0402 $^{a,b}$ | 0.97 $^{e}$ | 0.0360 $^{c,d,e}$ | 0.0463 $^{c}$ |
| V2F1G2 | 0.95 $^{b,c}$ | 0.0327 $^{a}$ | 0.0391 $^{b,c,d}$ | 1.18 $^{b}$ | 0.0395 $^{a}$ | 0.0470 $^{b,c}$ |
| V2F1G1 | 0.94 $^{b,c}$ | 0.0322 $^{a}$ | 0.0394 $^{a,b,c,d}$ | 0.96 $^{e}$ | 0.0375 $^{b,c}$ | 0.0463 $^{c}$ |
| V2F1G0 | 0.93 $^{c}$ | 0.0319 $^{a,b}$ | 0.0390 $^{c,d}$ | 0.84 $^{f,g,h}$ | 0.0355 $^{d,e,f}$ | 0.0448 $^{d}$ |
| V2F0G2 | 0.75 $^{f}$ | 0.0287 $^{d}$ | 0.0387 $^{c,d}$ | 1.09 $^{d}$ | 0.0377 $^{a,b,c}$ | 0.0465 $^{b,c}$ |
| V2F0G1 | 0.77 $^{e,f}$ | 0.0285 $^{d}$ | 0.0385 $^{d}$ | 0.87 $^{f}$ | 0.0347 $^{e,f}$ | 0.0441 $^{d}$ |
| V1F2G2 | 0.89 $^{d}$ | 0.0303 $^{c}$ | 0.0343 $^{e}$ | 1.14 $^{c}$ | 0.0367 $^{c,d}$ | 0.0411 $^{e}$ |
| V1F2G1 | 0.90 $^{d}$ | 0.0304 $^{b,c}$ | 0.0344 $^{e}$ | 0.96 $^{e}$ | 0.0352 $^{d,e,f}$ | 0.0393 $^{f}$ |
| V1F2G0 | 0.89 $^{d}$ | 0.0297 $^{c,d}$ | 0.0339 $^{e}$ | 0.82 $^{h}$ | 0.0340 $^{f,g}$ | 0.0387 $^{f}$ |
| V1F1G2 | 0.78 $^{e}$ | 0.0293 $^{c,d}$ | 0.0323 $^{f}$ | 0.95 $^{e}$ | 0.0365 $^{c,d,e}$ | 0.0388 $^{f}$ |
| V1F1G1 | 0.79 $^{e}$ | 0.0292 $^{c,d}$ | 0.0326 $^{f}$ | 0.83 $^{g,h}$ | 0.0354 $^{d,e,f}$ | 0.0371 $^{g}$ |
| V1F1G0 | 0.78 $^{e,f}$ | 0.0288 $^{c,d}$ | 0.0323 $^{f}$ | 0.72 $^{i}$ | 0.0329 $^{g,h}$ | 0.0358 $^{h}$ |
| V1F0G2 | 0.71 $^{g}$ | 0.0259 $^{e}$ | 0.0299 $^{g}$ | 0.86 $^{f,g}$ | 0.0313 $^{h,i}$ | 0.0359 $^{h}$ |
| V1F0G1 | 0.71 $^{g}$ | 0.0252 $^{e}$ | 0.0296 $^{g}$ | 0.73 $^{i}$ | 0.0305 $^{i}$ | 0.0339 $^{i}$ |
| $W_X$ | 0.097 | 0.056 | 0.093 | 0.107 | 0.065 | 0.089 |

[1] V, vegetative; F, flowering; G, grain-filling; 2, sufficient irrigation; 1, 50% sufficient irrigation; 0, no irrigation. [2] Different letters in columns indicate significant differences among treatments within a year at a 5% probability level using Duncan multiple range test.

The weight of seed vigor indices determined using the entropy weight method ranged from 0.056 to 0.161 (Figure 2 and Tables 5–7) in both years. The weighted grey relational grade determined by

GRA ($R_i^*$), seed vigor calculated by PCA ($P_i^*$) and CEM ($V_i$) are presented in Table 8. The highest values of $R_i^*$, $P_i^*$ and $V_i$ indicate the highest seed vigor evaluated by each method. The highest $V_i$ values of 0.805 and 0.863 were observed under V2F1G2 in 2018 and in V2F0G2 in 2019, respectively. Compared with values under V2F2G2 (control), $V_i$ increased by 7.3% and 1.6% in 2018 and 2019, respectively, under V2F1G2 and V2F0G2. The lowest $V_i$ values of 0.201 and 0.227 were observed under V1F0G1 in 2018 and 2019, respectively.

**Table 8.** Ranks of hybrid maize seed vigor under different irrigation treatments using principal component analysis (PCA), grey relational analysis (GRA) and combinatorial evaluation method (CEM) in 2018 and 2019.

| Treatment | 2018 | | | | 2019 | | | |
|---|---|---|---|---|---|---|---|---|
| | GRA(0.480) [2] | PCA(0.520) | CEM | | GRA(0.497) | PCA(0.503) | CEM | |
| | $R_i$* [3] | $P_i$* [4] | $V_i$ [5] | Rank | $R_i$* | $P_i$* | $V_i$ | Rank |
| V2F2G2 [1] | 0.723 | 0.774 | 0.750 | 6 | 0.816 | 0.882 | 0.849 | 3 |
| V2F2G1 | 0.711 | 0.749 | 0.731 | 8 | 0.622 | 0.660 | 0.641 | 4 |
| V2F2G0 | 0.709 | 0.760 | 0.735 | 7 | 0.492 | 0.418 | 0.454 | 9 |
| V2F1G2 | 0.730 | 0.873 | 0.805 | 1 | 0.792 | 0.913 | 0.853 | 2 |
| V2F1G1 | 0.698 | 0.845 | 0.774 | 5 | 0.587 | 0.658 | 0.623 | 5 |
| V2F1G0 | 0.703 | 0.850 | 0.780 | 3 | 0.470 | 0.405 | 0.438 | 12 |
| V2F0G2 | 0.799 | 0.777 | 0.788 | 2 | 0.846 | 0.881 | 0.863 | 1 |
| V2F0G1 | 0.779 | 0.778 | 0.779 | 4 | 0.525 | 0.523 | 0.524 | 8 |
| V1F2G2 | 0.484 | 0.468 | 0.475 | 12 | 0.553 | 0.585 | 0.569 | 6 |
| V1F2G1 | 0.485 | 0.463 | 0.474 | 13 | 0.467 | 0.415 | 0.441 | 11 |
| V1F2G0 | 0.477 | 0.446 | 0.461 | 14 | 0.387 | 0.181 | 0.283 | 14 |
| V1F1G2 | 0.479 | 0.523 | 0.502 | 9 | 0.535 | 0.601 | 0.568 | 7 |
| V1F1G1 | 0.477 | 0.515 | 0.497 | 10 | 0.419 | 0.302 | 0.360 | 13 |
| V1F1G0 | 0.467 | 0.491 | 0.480 | 11 | 0.351 | 0.106 | 0.228 | 15 |
| V1F0G2 | 0.338 | 0.088 | 0.208 | 15 | 0.462 | 0.432 | 0.447 | 10 |
| V1F0G1 | 0.334 | 0.078 | 0.201 | 16 | 0.359 | 0.097 | 0.227 | 16 |

[1] V, vegetative; F, flowering; G, grain-filling; 2, sufficient irrigation; 1, 50% sufficient irrigation; 0, no irrigation. [2] Numbers in parentheses indicate weights calculated by CEM, and described previously [36]. [3] $R_i^*$ is weighted grey relational grade, and calculated by Equation (10). [4] $P_i^*$ is the seed vigor calculated by PCA, and described previously [31]. [5] $V_i$ is the seed vigor calculated by a combinational value of each method, as was described by Jiang et al. [36].

Data analysis (Table 8) revealed that the highest seed vigor calculated by CEM was observed under treatments with V2F1G2 in 2018 and V2F0G2 in 2019, but decrease in yield by 6.3% in 2018 and 38.0% in 2019. The results showed that seed vigor and yield of hybrid maize cannot be improved at the same time under water deficit. Therefore, to ensure high yield and seed vigor of hybrid maize under drip irrigation, the optimal irrigation depth at different growth stages must be investigated in detail.

### *3.3. Water–Seed Vigor Model*

The crop water production function is often used to simulate crop yield based on the linear relationship between relative crop yield and relative evapotranspiration [36,48]. Figure 3b shows a linear relationship between relative seed vigor of hybrid maize evaluated by CEM ($V_i/V_{CK}$) and relative seasonal ET ($ET_i/ET_{CK}$), which is similar to relative yield in response to $ET_i/ET_{CK}$ (Figure 3a). Therefore, in this study, we used the crop water production functions to simulate the vigor of hybrid maize seeds under water deficit at different growth stages.

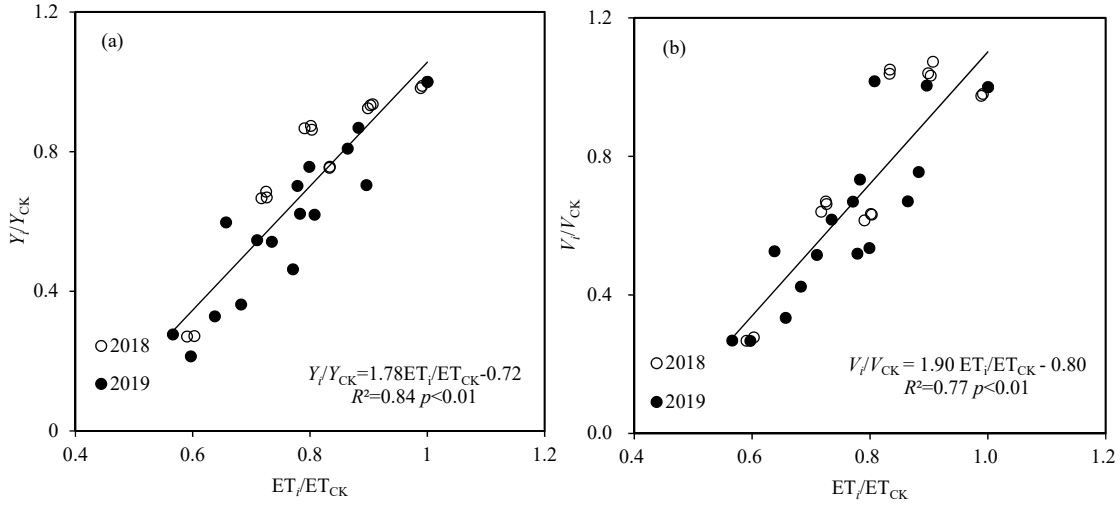


**Figure 3.** Linear relationships between relative yield ($Y_i/Y_{CK}$) and relative seasonal evapotranspiration ($ET_i/ET_{CK}$) (**a**), as well as relative seed vigor evaluated by a combinational evaluation method ($V_i/V_{CK}$) and $ET_i/ET_{CK}$ (**b**).

The calibration results of the water–seed vigor models are summarized in Table 9. For different models, $R^2$ and *RRMSE* were 0.65–0.88 and 0.132–0.175, respectively. The Rao model showed the best calibration results of $R^2$ = 0.88 and *RRMSE* = 0.132, and the water sensitivity indices at the vegetative, flowering, and grain-filling stages were 0.772, −0.343, and 0.916, respectively.

**Table 9.** The calibration results of seed vigor water sensitivity indices at the vegetative, flowering, and grain-filling stages for different models, calibrated using 12 irrigation treatments in 2018 and 2019. $R^2$, determination coefficients; *RRMSE*, relative root-mean-square error.

| Model | Water Sensitivity Index | | | $R^2$ | *RRMSE* |
|---|---|---|---|---|---|
| | Vegetative | Flowering | Grain-Filling | | |
| Blank | 0.379 | −0.217 | 0.807 | 0.65 | 0.175 |
| Steward | 0.615 | −0.136 | 0.811 | 0.85 | 0.140 |
| Rao | 0.772 | −0.343 | 0.916 | 0.88 | 0.132 |
| Jensen | 0.759 | 0.006 | 0.719 | 0.85 | 0.155 |
| Minhas | 2.184 | 0.352 | 1.437 | 0.84 | 0.154 |

The results of the water–seed vigor models validated using data of 20 irrigation treatments are presented in Figure 4. The results showed that althought the Rao model underestimated the measured value by 3%, it had the highest $R^2$, EF, and $d_{IA}$, and the lowest RRMSE and ARE. Therefore, the Rao model is recommended for predicting seed vigor of hybrid maize under water deficit with drip irrigation under film mulching in arid regions.

Because seed vigor is a complex trait, it is imperative to establish a model to predict seed vigor under water deficit. Compared with additive models, the multiplicative models are more physiologically meaningful. In this study, the Rao model is recommended for predicting seed vigor of hybrid maize under water deficit. The Rao model showed that water deficit at the grain-filling and vegetative stages reduced seed vigor, and seed vigor was more sensitive to water deficit at the grain-filling ($C_3$ = 0.916) than at the vegetative stage ($C_1$ = 0.772), whereas water deficit at the flowering stage increased seed vigor ($C_2$ = −0.343). Based on the results of previous studies, seed vigor is positively correlated with KW and SPC [70,72,76,77]. In this study, water deficit at the flowering stage increased KW and SPC (Table 4), thereby improving seed vigor. On the contrary, water deficit at the vegetative and grain-filling stages decreased of KW and SPC, thereby reducing seed vigor.

The water–seed vigor model can be used to optimize irrigation water management to ensure seed vigor of hybrid maize production under limited water availability.

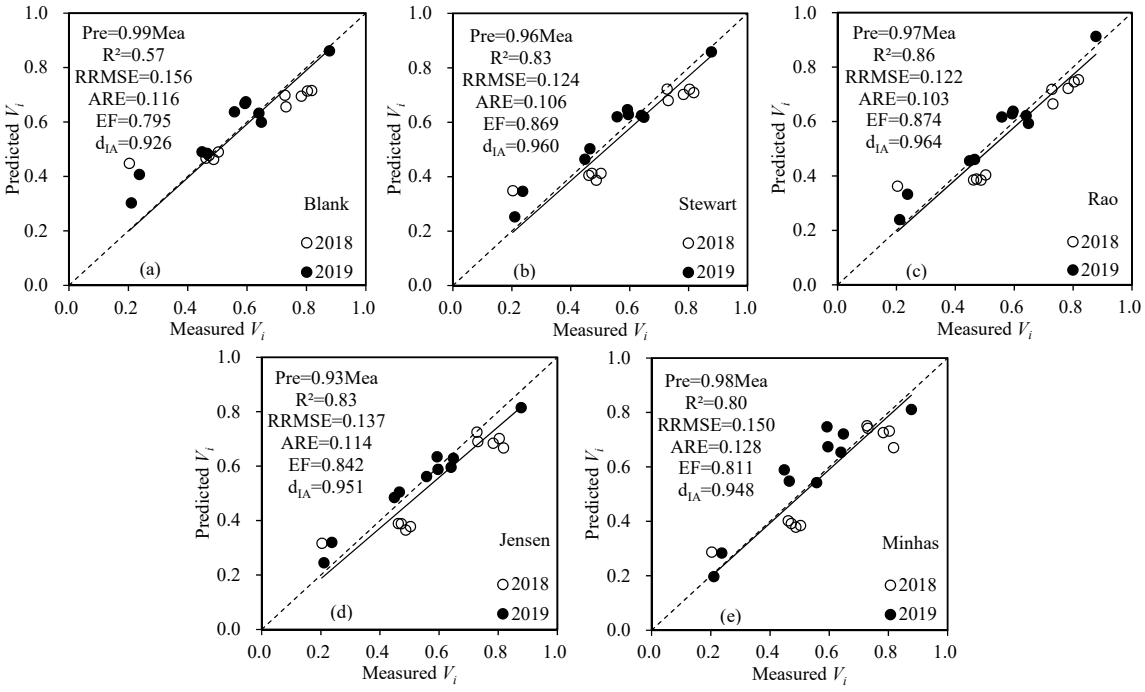


**Figure 4.** The validation results of the Blank (**a**), Stewart (**b**), Rao (**c**), Jensen (**d**), and Minhas (**e**) models. Model parameters were validated using data of 20 irrigation treatments in 2018 and 2019. The dotted line indicates the 1:1 line. $V_i$, seed vigor evaluated by combinational evaluation method; $R^2$, determination coefficients; RRMSE, relative root-mean-square error; ARE, average relative error; EF, modeling efficiency; $d_{\mathrm{IA}}$, agreement index.

## 4. Conclusions

The present study assessed the vigor of hybrid maize seeds that were produced under water deficit at different growth stages. Water deficit at different growth stages significantly decreased yield. Water deficit at the flowering stage increased SL, RL, and GI under different germination conditions. The seed vigor ranking of combinational evaluation method showed that V2F1G2 (sufficient irrigation at the vegetative and grain-filling stages and 50% of sufficient irrigation at the flowering stage) and V2F0G2 (sufficient irrigation at the vegetative and grain-filling stages and no irrigation at the flowering stage) produced higher seed vigor and reduced total irrigation volume by 17.7% and 19.3% in 2018 and 2019, respectively. The Rao model was superior to other models in predicting the vigor of hybrid maize seeds under water deficit. The results showed that an appropriate water deficit at the flowering stage could ensure seed vigor of hybrid maize production under limited water availability. Our research created a foundation for a water-saving irrigation strategy for hybrid maize production with drip irrigation under film mulching in an arid area.

**Author Contributions:** Conceptualization: T.D.; Formal analysis: R.S., T.D.; Investigation: R.S., L.T.; Methodology: R.S.; Supervision: T.D., M.K.S.; Writing—original draft: R.S.; Writing—review and editing: T.D., M.K.S. All authors have read and agreed to the published version of the manuscript.

**Funding:** This work was funded in part by the National Natural Science Foundation of China (51725904, 51621061, and 51861125103), the Research Projects of Agricultural Public Welfare Industry in China (201503125), and the Discipline Innovative Engineering Plan (111 Program, B14002).

**Acknowledgments:** The authors are grateful to the editors and reviewers for leveraging the quality. The authors also thank the NMSU Agricultural Experiment Station for support.

**Conflicts of Interest:** The authors declare no conflict of interest.

## References


1. Denis, T.; Gales, D.; Chiriac, G.; Răus, L.; Jităreanu, G. Impact of plowing on some soil physical properties under hybrid seed corn production. *ProEnvironment/ProMediu* **2013**, *6*, 183–186.
2. Venkatesh, T.V.; Breeze, M.L.; Liu, K.; Harrigan, G.G.; Culler, A.H. Compositional analysis of grain and forage from MON 87427, an inducible male sterile and tissue selective glyphosate-tolerant maize product for hybrid seed production. *J. Agric. Food Chem.* **2014**, *62*, 1964–1973. [CrossRef] [PubMed]
3. Benke, Z. The Corn Seed Production in Hungary in the Last 60 Years. In *60 Years of Hungarian Hybrid Maize 1953-2013, Proceedings of the Hybrid Maize Conference, Martonvasar, Hungary, 14 November 2013*; Marton, L.C., Spitko, T., Eds.; Pannonian Plant Biotechnology Association: Martonvasar, Hungary, 2013.
4. Arisnabarreta, S.; Solari, F. Hybrid maize seed production yield associations with inbred line performance in multienvironment trials. *Crop Sci.* **2017**, *57*, 3203–3216. [CrossRef]
5. Perry, D.A. Report of the vigour test committee 1974–1977. *Seed Sci. Technol.* **1978**, *6*, 159–181.
6. Dalil, B.; Ghassemi-Golezani, K.; Moghaddam, M.; Raey, Y. Effects of seed viability and water supply on leaf chlorophyll content and grain yield of maize (*Zea mays*). *J. Food Agric. Environ.* **2010**, *8*, 399–402.
7. Woodstock, L.W. Physiological and biochemical tests for seed vigor. *Seed Sci. Technol.* **1973**, *1*, 127–157.
8. ISTA. International rules for seed testing. *Proc. Int. Seed Test. Assoc.* **1985**, *31*, 1–152.
9. Noli, E.; Casarini, E.; Urso, G.; Conti, S. Suitability of three vigour test procedures to predict field performance of early sown maize seed. *Seed Sci. Technol.* **2008**, *36*, 168–176. [CrossRef]
10. Basu, S.; Sharma, S.P.; Dadlani, M. Storability studies on maize (*Zea mays* L.) parental line seeds under natural and accelerated ageing conditions. *Seed Sci. Technol.* **2004**, *32*, 239–245. [CrossRef]
11. Lovato, A.; Noli, E.; Lovato, A.F.S. The relationship between three cold test temperatures, accelerated ageing test and field emergence of maize seed. *Seed Sci. Technol.* **2005**, *33*, 249–253. [CrossRef]
12. Chen, Y.; Burris, J.S. Role of carbohydrates in desiccation tolerance and membrane behavior in maturing maize seed. *Crop Sci.* **1990**, *30*, 971–975. [CrossRef]
13. Bailly, C.; Benamar, A.; Corbineau, F.; Côme, D. Changes in malondialdehyde content and in superoxide dismutase, catalase and glutathione reductase activities in sunflower seeds as related to deterioration during accelerated aging. *Physiol. Plant.* **1996**, *97*, 104–110. [CrossRef]
14. Zhao, G.W.; Sun, Q.; Wang, J.H. Improving seed vigour assessment of super sweet and sugar-enhanced sweet corn (*Zea mays* saccharata). *New Zeal. J. Crop Hortic. Sci.* **2007**, *35*, 349–356. [CrossRef]
15. Usha, T.N.; Malavika, D. Evaluation of seed vigour in onion. *Seed Res.* **2009**, *37*, 106–114.
16. Mao, J.; Chen, H.; Gu, X.; Yu, Y.; Hu, J. Comprehensive evaluation of seed vigor in sweet corn germplasm. *J. Agric.* **2016**, *6*, 6–11. (In Chinese with English abstract)
17. Dornbos, D.L.; Mullen, R.E.; Shibles, R.E. Drought stress effects during seed fill on soybean seed germination and vigor. *Crop Sci.* **1989**, *29*, 476–480. [CrossRef]
18. Smiciklas, K.D.; Mullen, R.E.; Carlson, R.E.; Knapp, A.D. Soybean seed quality response to drought stress and pod position. *Agron. J.* **1992**, *84*, 166–170. [CrossRef]
19. Vieira, R.D.; TeKrony, D.M.; Egli, D.B. Effect of drought and defoliation stress in the field on soybean seed germination and vigor. *Crop Sci.* **1992**, *32*, 471–475. [CrossRef]
20. Heatherly, L.G. Drought stress and irrigation effects on germination of harvested soybean seed. *Crop Sci.* **1993**, *33*, 777–781. [CrossRef]
21. Samarah, N.H.; Mullen, R.E.; Anderson, I. Soluble sugar contents, germination, and vigor of soybean seeds in response to drought stress. *J. New Seeds* **2009**, *10*, 63–73. [CrossRef]
22. Eskandari, H.; Alizadeh-Amraie, A.; Kazemi, K. Effect of planting pattern and irrigation system on germination performance of maize seeds harvested at different times of maturation. *Seed Sci. Technol.* **2018**, *46*, 371–375. [CrossRef]
23. Zhang, J.; Cheng, Z.; Zhang, R. Regulated deficit drip irrigation influences on seed maize growth and yield under film. *Procedia Eng.* **2012**, *28*, 464–468.
24. Wang, J.; Tong, L.; Kang, S.; Li, F.; Zhang, X.; Ding, R.; Du, T.; Li, S. Flowering characteristics and yield of maize inbreds grown for hybrid seed production under deficit irrigation. *Crop Sci.* **2017**, *57*, 2238–2250. [CrossRef]

25. Ran, H.; Kang, S.; Li, F.; Du, T.; Ding, R.; Li, S.; Tong, L. Responses of water productivity to irrigation and N supply for hybrid maize seed production in an arid region of Northwest China. *J. Arid Land.* **2017**, *9*, 504–514. [CrossRef]
26. Yuan, C.; Feng, S.; Huo, Z.; Ji, Q. Effects of deficit irrigation with saline water on soil water-salt distribution and water use efficiency of maize for seed production in arid Northwest China. *Agric. Water Manag.* **2019**, *212*, 424–432. [CrossRef]
27. Ghassemi-Golezani, K.; Soltani, A.A. The effect of water limitation in the field on seed quality of maize and sorghum. *Seed Sci. Technol.* **1997**, *25*, 321–323.
28. Takele, A.; Farrant, J. Seed germination and storage reserves of maize and sorghum after exposure to and recovery from pre- and post-flowering dehydration. *Acta Agron. Hungarica.* **2010**, *58*, 133–142. [CrossRef]
29. Ghassemi-golezani, K.; Heydari, S.; Hassannejad, S. Seed vigor of maize (*Zea mays*) cultivars affected by position on ear and water stress. *Azarian J. Agric.* **2015**, *2*, 40–45.
30. Baber, S.A.; Waseem, B.; Loangove, M.A. Influence of different irrigation scheduling practices on the growth and yield performance of maize (*Zea mays* L.) variety Agaiti-2002. *J. Biol. Agric. Healthc.* **2015**, *5*, 168–174.
31. Wang, C.; Gu, F.; Chen, J.; Yang, H.; Jiang, J.; Du, T.; Zhang, J. Assessing the response of yield and comprehensive fruit quality of tomato grown in greenhouse to deficit irrigation and nitrogen application strategies. *Agric. Water Manag.* **2015**, *161*, 9–19. [CrossRef]
32. Wei, Z.; Du, T.; Li, X.; Fang, L.; Liu, F. Interactive effects of elevated $CO_2$ and N fertilization on yield and quality of tomato grown under reduced irrigation regimes. *Front. Plant Sci.* **2018**, *9*, 1–10. [CrossRef] [PubMed]
33. Wang, F. Response of Greenhouse Tomato Yield and Quality to Water Stress and the Irrigation Index for Water Saving & Fruit Quality Improving. Ph.D. Thesis, China Agricultural University, Beijing, China, 2011.
34. Ding, X.; Chong, X.; Bao, Z.; Xue, Y.; Zhang, S. Fuzzy comprehensive assessment method based on the entropy weight method and its application in the water environmental safety evaluation of the Heshangshan drinking water source area, three gorges reservoir area, China. *Water* **2017**, *9*, 329. [CrossRef]
35. Wang, J.; Kang, S.; Zhang, X.; Du, T.; Tong, L.; Ding, R.; Li, S. Simulating kernel number under different water regimes using the Water-Flowering Model in hybrid maize seed production. *Agric. Water Manag.* **2018**, *209*, 188–196. [CrossRef]
36. Jiang, X.; Zhao, Y.; Tong, L.; Wang, R.; Zhao, S. Quantitative analysis of tomato yield and comprehensive fruit quality in response to deficit irrigation at different growth stages. *HortScience* **2019**, *54*, 1409–1417. [CrossRef]
37. Guo, S.; Wang, J.; Zhang, F.; Wang, Y.; Guo, P. An integrated water-saving and quality-guarantee uncertain programming approach for the optimal irrigation scheduling of seed maize in arid regions. *Water* **2018**, *10*, 908. [CrossRef]
38. Paredes, P.; Rodrigues, G.C.; Alves, I.; Pereira, L.S. Partitioning evapotranspiration, yield prediction and economic returns of maize under various irrigation management strategies. *Agric. Water Manag.* **2014**, *135*, 27–39. [CrossRef]
39. Li, X.; Zhang, X.; Niu, J.; Tong, L.; Kang, S.; Du, T.; Li, S.; Ding, R. Irrigation water productivity is more influenced by agronomic practice factors than by climatic factors in Hexi Corridor, Northwest China. *Sci. Rep.* **2016**, *6*, 1–10. [CrossRef]
40. Allen, R.G.; Pereira, L.S.; Raes, D.; Smith, M. *Crop Evapotranspiration: Guidelines for Computing Crop Water Requirements: FAO Irrigation and Drainage Paper 56*; FAO-Food and Agriculture Organization of the United Nations: Rome, Italy, 1998; p. 300.
41. Jiang, X.; Kang, S.; Tong, L.; Li, F.; Li, D.; Ding, R.; Qiu, R. Crop coefficient and evapotranspiration of grain maize modified by planting density in an arid region of northwest China. *Agric. Water Manag.* **2014**, *142*, 135–143. [CrossRef]
42. Simonne, A.H.; Simonne, E.H.; Eitenmiller, R.R.; Mills, H.A.; Cresman, C.P., III. Could the Dumas method replace the Kjeldahl digestion for nitrogen and crude protein. *J. Sci. Food Agric.* **1997**, *73*, 39–45. [CrossRef]
43. Madhava Rao, K.V.; Sresty, T.V.S. Antioxidative parameters in the seedlings of pigeonpea (*Cajanus cajan* (L.) Millspaugh) in response to Zn and Ni stresses. *Plant Sci.* **2000**, *157*, 113–128. [CrossRef]
44. Shannon, L.M.; Kay, E.; Lew, J.Y. Peroxidase isozymes from horseradish roots. I. Isolation and physical properties. *J. Biol. Chem.* **1966**, *241*, 2166–2172. [PubMed]
45. Sedmak, J.J.; Grossberg, S.E. A rapid, sensitive, and versatile assay for protein using Coomassie brilliant blue G250. *Anal. Biochem.* **1977**, *79*, 544–552. [CrossRef]

46. Blank, H.G. Optimal irrigation decisions with limited water. Ph.D. Thesis, Colorado State University, Fort Collins, CO, USA, 1975.
47. Stewart, J.I.; Misra, R.D.; Puritt, W.O.; Hagan, R.M. Irrigating corn and grain sorghum with a deficient water supply. *Trans. Am. Soc. Agric. Eng.* **1975**, *18*, 270–280. [CrossRef]
48. Rao, N.H.; Sarma, P.B.S.; Chander, S. A simple dated water-production function for use in irrigated agriculture. *Agric. Water Manag.* **1988**, *13*, 25–32. [CrossRef]
49. Jensen, M.E. *Water Consumption by Agricultural Plants*; Kozlowski, T.T., Ed.; Academic Press: New York, NY, USA, 1968; pp. 1–22.
50. Minhas, B.S.; Parikh, K.S.; Srinivasan, T.N. Toward the structure of production function for wheat yields with dated inputs of irrigation water. *Water Resour. Res.* **1974**, *10*, 383–393. [CrossRef]
51. Nesmith, D.S.; Ritchie, J.T. Effects of soil water-deficits during tassel emergence on development and yield component of maize (*Zea mays*). *Field Crops Res.* **1992**, *28*, 251–256. [CrossRef]
52. NeSmith, D.S.; Ritchie, J.T. Short- and long-term responses of corn to a pre-anthesis soil water deficit. *Agron. J.* **1992**, *84*, 699–704. [CrossRef]
53. Setter, T.L.; Flannigan, B.A.; Melkonian, J. Loss of kernel set due to water deficit and shade in maize: Carbohydrate supplies, abscisic acid, and cytokinins. *Crop Sci.* **2001**, *41*, 1530–1540. [CrossRef]
54. Hammad, H.M.; Ahmad, A.; Abbas, F.; Farhad, W.; Cordoba, B.C.; Hoogenboom, G. Water and nitrogen productivity of maize under semiarid environments. *Crop Sci.* **2015**, *55*, 877–888. [CrossRef]
55. Pandey, R.K.; Maranville, J.W.; Admou, A. Deficit irrigation and nitrogen effects on maize in a Sahelian environment I. Grain yield and yield components. *Agric. Water Manag.* **2000**, *46*, 1–13. [CrossRef]
56. Çakir, R. Effect of water stress at different development stages on vegetative and reproductive growth of corn. *Field Crops Res.* **2004**, *89*, 1–16. [CrossRef]
57. Lu, D.; Cai, X.; Zhao, J.; Shen, X.; Lu, W. Effects of drought after pollination on grain yield and quality of fresh waxy maize. *J. Sci. Food Agric.* **2015**, *95*, 210–215. [PubMed] [CrossRef] [PubMed]
58. Oktem, A. Effect of water shortage on yield, and protein and mineral compositions of drip-irrigated sweet corn in sustainable agricultural systems. *Agric. Water Manag.* **2008**, *95*, 1003–1010. [CrossRef]
59. Ertek, A.; Kara, B. Yield and quality of sweet corn under deficit irrigation. *Agric. Water Manag.* **2013**, *129*, 138–144. [CrossRef]
60. Harder, H.J.; Carlson, R.E.; Shaw, R.H. Leaf photosynthetic response to foliar fertilizer applied to corn plants during grain fill. *Agron. J.* **1982**, *74*, 759–761. [CrossRef]
61. Aydinsakir, K.; Erdal, S.; Buyuktas, D.; Bastug, R.; Toker, R. The influence of regular deficit irrigation applications on water use, yield, and quality components of two corn (*Zea mays* L.) genotypes. *Agric. Water Manag.* **2013**, *128*, 65–71. [CrossRef]
62. Koca, Y.O.; Canavar, O.; Yorulmaz, A.; Erekul, O. Influence of nitrogen level and water scarcity during seed filling period on seed yield and fatty acid compositions of corn. *Crop Sci.* **2015**, *40*, 90–97.
63. Anwar, S.; Iqbal, M.; Akram, H.M.; Niaz, M.; Rasheed, R. Influence of drought applied at different growth stages on kernel yield and quality in maize (*Zea Mays* L.). *Commun. Soil Sci. Plant Anal.* **2016**, *47*, 2225–2232. [CrossRef]
64. Borrás, L.; Curá, J.A.; Otegui, M.E. Maize kernel composition and post-flowering source-sink ratio. *Crop Sci.* **2002**, *42*, 781–790.
65. Seebauer, J.R.; Singletary, G.W.; Krumpelman, P.M.; Ruffo, M.L.; Below, F.E. Relationship of source and sink in determining kernel composition of maize. *J. Exp. Bot.* **2010**, *61*, 511–519. [CrossRef]
66. Jumrani, K.; Bhatia, V.S. Combined effect of high temperature and water-deficit stress imposed at vegetative and reproductive stages on seed quality in soybean. *Indian J. Plant Physiol.* **2018**, *23*, 227–244. [CrossRef]
67. Lieffering, M.; Andrews, M.; McKenzie, B.A. Nitrate stimulation of mobilization of seed reserves in temperate cereals: Importance of water uptake. *Ann. Bot.* **1996**, *78*, 695–701. [CrossRef]
68. Hara, Y.; Toriyama, K. Seed nitrogen accelerates the rates of germination, emergence, and establishment of rice plants. *Soil Sci. Plant Nutr.* **1998**, *44*, 359–366. [CrossRef]
69. Bulisani, E.A.; Warner, R.L. Seed protein and nitrogen effects upon seedling vigor in wheat. *Agron. J.* **1980**, *72*, 657–662. [CrossRef]
70. Ries, S.K.; Everson, E.H. Protein content and seed size relationships with seedling vigor of wheat cultivars. *Agron. J.* **1973**, *65*, 884–886. [CrossRef]

71. Wen, D.; Hou, H.; Meng, A.; Meng, J.; Xie, L.; Zhang, C. Rapid evaluation of seed vigor by the absolute content of protein in seed within the same crop. *Sci. Rep.* **2018**, *8*, 1–8. [CrossRef] [PubMed]
72. Ambika, S.; Manonmani, V.; Somasundaram, G. Review on effect of seed size on seedling vigour and seed yield. *Res. J. Seed Sci.* **2014**, *7*, 31–38. [CrossRef]
73. Al-Karaki, G.N. Seed size and water potential effects on water uptake, germination and growth of lentil. *J. Agron. Crop Sci.* **1998**, *181*, 237–242. [CrossRef]
74. Roy, S.K.S.; Hamid, A.; Giashuddin Miah, M.; Hashem, A. Seed size variation and its effects on germination and seedling vigour in rice. *J. Agron. Crop Sci.* **1996**, *176*, 79–82. [CrossRef]
75. da Silva, R.T.; de Oliveira, A.B.; Lopes, M.F.Q.; Guimarães, A.; Dutra, A.S. Physiological quality of sesame seeds produced from plants subjected to water stress. *Rev. Cienc. Agron.* **2016**, *47*, 643–648. [CrossRef]
76. Ghooshchi, F.; Reza, H.; Moghaddam, T. Evaluation of germination and emergence behaviors of rapeseed (*Brassica napus* L.) cultivars under limited irrigation. *Am. J. Agric. Environ. Sci.* **2013**, *13*, 174–184.
77. Pedrinho, A.; Mariano, E.; Merloti, L.F.; de Sa, M.E. Common bean seed quality as affected by cover crop mixtures and nitrogen fertilization. *Aust. J. Crop Sci.* **2019**, *13*, 300–308. [CrossRef]
78. Eisvand, H.R.; Moori, S.; Ismaili, A.; Sasani, S. Effects of late-season drought stress on physiology of wheat seed deterioration: Changes in antioxidant enzymes and compounds. *Seed Sci. Technol.* **2016**, *44*, 327–341. [CrossRef]